



MODELING AND NUMERICAL SIMULATION OF ELASTO-VISCOPLASTIC ANISOTROPIC BEHAVIOR OF TANTALUM INCLUDING THE DUCTILE DAMAGE EFFECT

THOMAS PARIS^{1,2}, KHÉMAÏS SAANOUNI¹, MANUEL FRANCOIS¹, DAMIEN DELAPLANCHE²

¹ *University of Technology of Troyes, ICD/LASMIS, CNRS, FRE 2848 BP 2060 10010 Troyes, France*

² *CEA Valduc, LCS1 21120 Is-sur-Tille, France*

Corresponding author thomas.paris@utt.fr (T. Paris)

Abstract

At room temperature, the tantalum is shown to exhibit a high and typical strain rate sensitivity. Various experimental tests including uniaxial tensile tests for the three in-plane directions, relaxation and cyclic shear tests have been conducted at room temperature in order to study the mechanical behavior of tantalum. Based on this experimental data, an elasto-viscoplastic model is developed including the initial viscoplastic anisotropy as well as the isotropic ductile damage effect. Using the framework of the thermodynamics with state variables, an appropriate state and dissipation potentials are proposed to account for, the initial viscoplastic flow anisotropy, the mixed non linear isotropic and kinematic hardenings and the isotropic ductile damage effects. Specific developments are made to introduce different isotropic type hardenings thanks to the coupling between accumulative plastic strain and the viscous or kinematic stresses. The proposed model, implemented into ABAQUS/EXPLICIT via the user subroutine Vumat, is used to simulate different experimental tests in order to determine the accurate values of the overall material parameters. The special treatment of the plane stress is addressed and allows inherently to describe anisotropic behavior. Finally, some simple 2D and 3D simulations of deep drawing tests are carried out to validate the accuracy of the proposed model.

Key words: viscoplasticity, anisotropy, damage, plane stress, tantalum, finite element analysis

1. CONSTITUTIVE EQUATIONS

The formulation of elasto-viscoplastic model is based on the thermodynamical framework and uses different state variables to describe phenomena such as isotropic and kinematic hardening, viscous and damage effects [8–10]. These state variables are,

- ($\underline{\varepsilon}^{vp}, \underline{\sigma}$) : visco-plastic strain and stress tensors
 ($\underline{\alpha}, \underline{X}$) : kinematic hardening strain and stress tensors
 (r, R) : isotropic hardening strain and stress
 (D, Y) : isotropic damage and its associated force
- (1)

State relations

$$\underline{\sigma} = (1 - D) \underline{\underline{\Lambda}} : \underline{\varepsilon}^e \quad (2)$$

$$\underline{\underline{\Lambda}} = 2\mu \underline{\underline{1}} + \lambda \underline{\underline{1}} \otimes \underline{\underline{1}} \text{ in the isotropic case}$$

$$\underline{X} = (1 - D) \frac{2}{3} C \underline{\alpha} \quad (3)$$

$$R = (1 - D) Q r \quad (4)$$

$$Y = \frac{1}{2} \underline{\varepsilon}^e : \underline{\underline{\Lambda}} : \underline{\varepsilon}^e + \frac{1}{3} C \underline{\alpha} : \underline{\alpha} + \frac{1}{2} Q r^2 \quad (5)$$

State equations are derived from the state potential (Helmholtz free energy) and evolution equations come from the dissipation potential. This leads to:

Evolution equations

$$\dot{\alpha} = \dot{\lambda}^{vp} \left(\frac{n}{\sqrt{1-D}} - a\alpha \right) \quad (6)$$

$$\dot{r} = \dot{\lambda}^{vp} \left(\frac{1}{\sqrt{1-D}} - br \right) \quad (7)$$

$$\dot{\varepsilon}^p = \dot{\lambda}^{vp} \frac{n}{\sqrt{1-D}} \quad (8)$$

$$\dot{D} = \frac{\dot{\lambda}^{vp}}{(1-D)^{\beta+\frac{1}{2}}} \left\langle \frac{Y - Y_0}{S} \right\rangle^s \quad (9)$$

Where (λ, μ) are the classical Lamé's constants; (C, a) and (Q, b) are two couples of parameters for kinematic and isotropic hardenings and S, s, β, Y_0 are damage parameters. The viscoplastic "multiplier" is given by [7],

$$\dot{\lambda}^{vp} = K_1 \sinh \left\langle \frac{f}{K_2} \right\rangle \quad (10)$$

where (K_1, K_2) are parameters characterizing the material viscosity and f is the yield function of von Mises type given by,

$$f(\underline{\sigma}, \underline{X}, R, D) = \frac{\|\underline{\sigma} - \underline{X}\| - R}{\sqrt{1-D}} - \sigma_y \leq 0 \quad (11)$$

in which σ_y is the yield stress.

The above constitutive equations are obtained following the thermodynamic method as can be found in [8–10]. However, some modification should be introduced in order to better describe the tantalum (Ta) behavior.

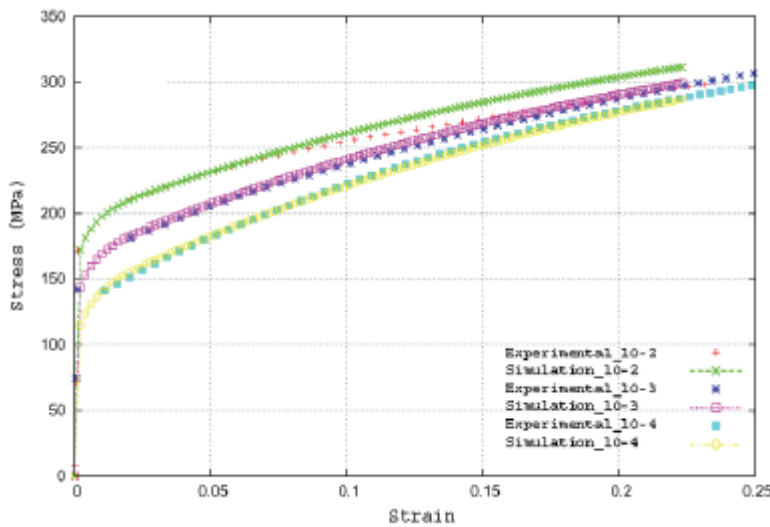


Fig. 1. Tensile test, comparison between experimental and simulation for different strain rate, from $\dot{\varepsilon} = 10^{-4} s^{-1}$ to $\dot{\varepsilon} = 10^{-2} s^{-1}$.

2. APPLICATION TO TANTALUM

2.1. Viscosity effect

Viscosity effects are well described by a hyperbolic sine function as proposed by Delobelle [3–5]. This is especially efficient to describe high strain rate saturation that Norton power law is enable to model. Most commonly, the stress strain curves at different strain rates are equidistant for bcc alloys while the gap is increasing with strain in fcc alloys [1]. Away from this consideration, various unusual rate sensitivities can be observed and this is especially the case of the tantalum rate dependency. As can be seen experimentally, Ta viscosity is really dependent of plastic strain level and the more the plastic strain the less the viscosity. Moreover, tensile tests show an initial drop in stress followed by inelastic strain at constant stress typical of Lüders band occurrence. This phenomenon is a consequence of dislocation unlocking, solute dragging by dislocations, etc [2]. The amplitude between high and low stress levels is increasing with strain rate.

To model this specific behavior, the drag stress K_2 , see equation 10, is taken function of accumulated plastic strain p .

$$K_2 = \left(K_m + (K_M - K_m)e^{-K_{ov}p} \right) e^{-K_v p} \quad (12)$$

Where K_m, K_M, K_{ov}, K_v are material parameters that describe the coupling effect. For simplicity, Lüders pick on the experimental stress-strain curve (figure 1) is removed. Putting $K_{ov} = 0$, the two main parameters that describe viscosity effect are K_M and K_v and this is enough to give a good agreement with experimental data. For a given deformation (here $\epsilon = 10^{-1}$), a relaxation test shows that the amount of viscous stress is well evaluated by the model (figure 2).

2.2. Isotropic and kinematic hardenings coupling

The cyclic hardening or softening is generally modeled by the isotropic hardening evolution but could also be caught by a coupling between the kinematic hardening and the isotropic hardening represented by the accumulated plastic strain (p) [6]. To better describe the cyclic shear behavior of Ta, the state equation of kinematic hardening is rewritten as,



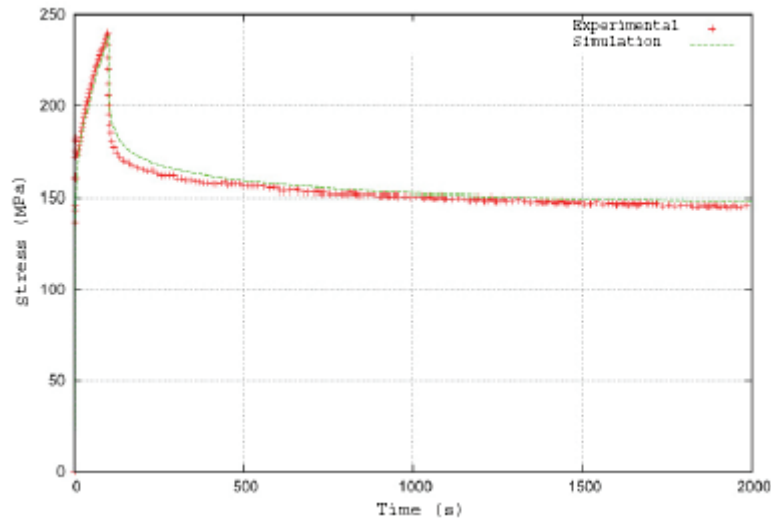


Fig. 2. Relaxation test, comparison between experimental and simulation for strain rate.

$$\underline{\Sigma} = (1 - D) \frac{2}{3} C(p) \underline{\alpha} \quad (13)$$

$$C(p) = C_0 + (C_\infty + C_0)(1 - e^{-\phi p}) \quad (14)$$

are compared with the corresponding simulations as indicated in figure 4.

2.4. Deep drawing test

To show the model accuracy in both 2D and 3D cases, the deep drawing test of cylindrical cup, presented in figure 5, is worked out.

For the same test, 2D and 3D force-displacement responses are very closed. The 2D simulation overestimates the maximum loading force of about 3%. This gap starts from a displacement of 6 mm and continue to grow up to failure. Moreover, the total failure of the blank is well described in time and space, since the failure time and location are almost the same between 2D and 3D.

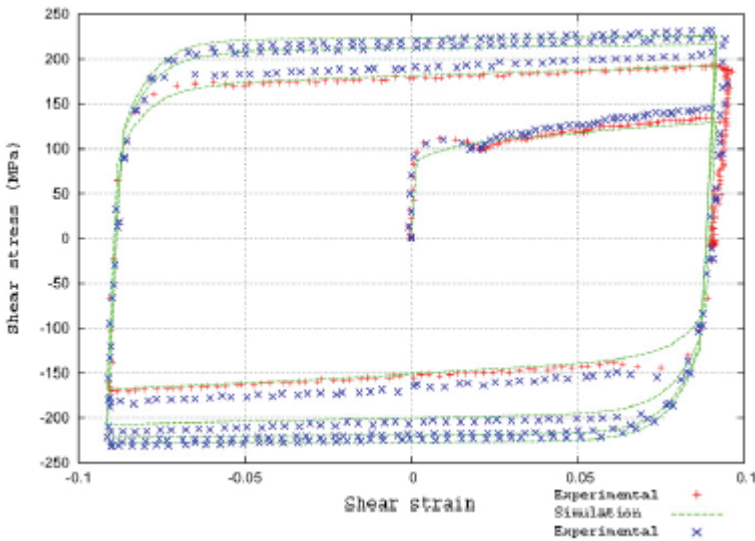


Fig. 3. Shear test, comparison between experimental and simulation for shear strain rate $\dot{\gamma} = \sqrt{3} \cdot 10^{-3} s^{-1}$ at $\pm 9 \cdot 10^{-2}$ for four cycles.

As shown in figure 3, this modification leads to a good agreement with experimental stress-strain loops for four successive cycles.

2.3. Anisotropy effect

The special case of the plane stress is treated thanks to a projection based algorithm [11] and allows inherently describing anisotropic behavior. Consequently, it's possible to recover a quadratic form of anisotropic criterion with the equation formulated before. Three in-plane uniaxial tensile tests

3. CONCLUSION

An elasto-viscoplastic model has been extended to simulate the initial viscoplastic anisotropy as well as the isotropic ductile damage effect of tantalum. Examples of parameters identification on various experimental data base are presented and a good agreement can be found between experimental and simulated results showing the ability of the model to catch specific mechanical effects of such a material including the fracture occurrence.



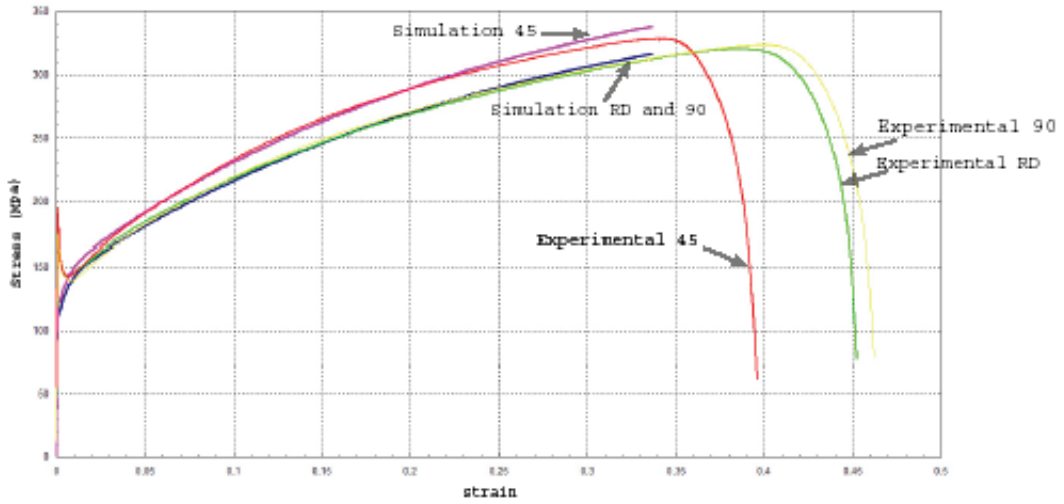


Fig. 4. Tensile test, comparison between experimental and simulation in three direction in-plane for strain rate equal to $\dot{\epsilon} = 10^{-4} s^{-1}$. RD refers to rolling direction, 45 and 90.

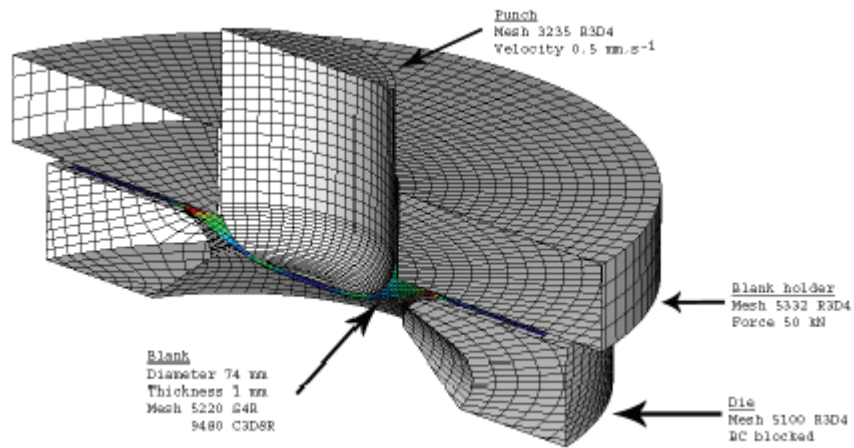


Fig. 5. Schematic representation of deep drawing test with boundary conditions.

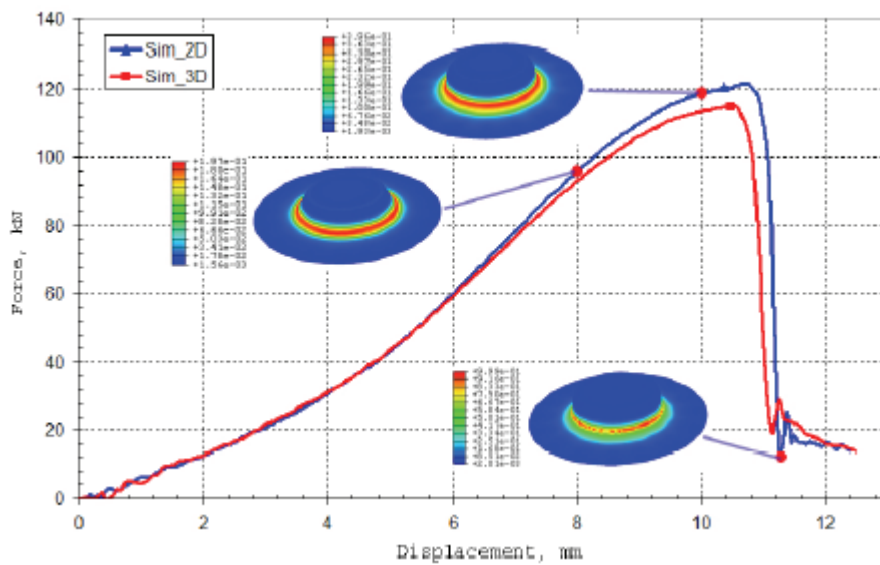


Fig. 6. Comparison between force-displacement responses of 2D and 3D cases for the deep drawing test and damage distribution for three steps of the 2D simulation.



ACKNOWLEDGEMENTS

The technical and financial supports of the CEA Valduc (France) is gratefully acknowledged.

REFERENCES

1. Chen, S., Kocks, U., High temperature plasticity in copper polycrystals, in: Freed W. K., A.D (ed.), High Temperature Constitutive Modeling, Theory and Applications, ASME, 1991.
2. Cottrell, A., Bilby, B., Dislocation theory of yielding and strain ageing of iron, Proc. Phys. Soc. London, Sec. A62, 1949, 49–62.
3. Delobelle, P., Synthesis of the elastoviscoplastic behavior and modelization of an austenitic stainless steel over a large temperature range, under uniaxial and biaxial loadings, part I Behavior, Int. J. of Plasticity, 9, 1993, 65–85.
4. Delobelle, P., Synthesis of the elastoviscoplastic behavior and modelization of an austenitic stainless steel over a large temperature range, under uniaxial and biaxial loadings, part II Phenomenological modelization, Int. J. of Plasticity, 9, 1993, 87–118.
5. Delobelle, P., Robinet, P., Bocher, L., Experimental study and phenomenological modelization of ratcheting under uniaxial and biaxial loading on an austenitic stainless steel, Int. J. of Plasticity, 11, 1995, 295–330.
6. Marquis, D., Etude théorique et vérification expérimentale d'un modèle de plasticité cyclique, Master's thesis, Université Pierre et Marie Curie, Paris 6, 1979.
7. Paris, T., Modélisation du comportement mécanique des liaisons soudées hétérogènes ta/ta6v : Comportement et critère de rupture, Ph.D. thesis, Université de Technologie de Troyes, 2008.
8. Saanouni, K., Sur l'analyse de la fissuration des milieux elasto-viscoplastiques par la théorie de l'endommagement continu, Ph.D. thesis, Université de Technologie de Compiègne, 1988.
9. Saanouni, K., Chaboche, J., Computational damage mechanics. application to metal forming, numerical and computational methods, Elsevier Oxford, 3(7), 2003, 321–376.
10. Saanouni, K., Forster, C., BenHatira, F., On the inelastic flow with damage, Int. J. Damage Mech, 3(2), 1994, 140–169.
11. Simo, J., Taylor, R., A return mapping algorithm for plane stress elastoplasticity, Int. J. Num. Meth. Engng., 22, 1986, 649–670.

MODELOWANIE I SYMULACJA NUMERYCZNA
SPRĘŻYSTO LEPKO PLASTYCZNEGO
ANIZOTROPOWEGO ZACHOWANIA TANTALU
Z UWZGLĘDNIENIEM EFEKTU PLASTYCZNEGO
PĘKANIA

Streszczenie

W temperaturze pokojowej tantal wykazuje typową wysoką wrażliwość na prędkość odkształcenia. Szereg testów, w tym jednoosiowy test rozciągania, relaksacji i cykliczny test ścinania, zostało przeprowadzonych w temperaturze pokojowej w celu poznania mechanicznych własności tantal. Bazując na otrzymanych danych eksperymentalnych opracowano sprężysto lepkoplastyczny model uwzględniający początkową lepkoplastyczną anizotropię jak również izotropowy efekt lepkoplastycznego pęknięcia. Wykorzystując termodynamiczne podejście ze zmiennymi stanu zostały zaproponowane zmienne stanu i potencjały dyssypacyjne aby uwzględnić anizotropię w początkowym lepkoplastycznym płynięciu, oraz aby połączyć nieliniowe izotropowe i kinematyczne modele umocnienia oraz efekty lepkoplastycznego pęknięcia. Szczególny nacisk położono na opracowanie złożonych modeli umocnienia materiału. Opracowany model zaimplementowano w programie ABAQUS/EXPLICIT przez procedurę użytkownika Vumant. Model ten został wykorzystany do symulacji różnych testów w celu identyfikacji dokładnych wartości parametrów materiałowych. W pracy przedstawiono również wyniki prostych symulacji w 2D i 3D testów głębokiego tłoczenia przeprowadzone w celu weryfikacji poprawności proponowanego modelu.

Submitted: September 30, 2008

Submitted in a revised form: November 17, 2008

Accepted: November 17, 2008

